

Agnieszka Pawlak<sup>1</sup> and David W. Eaton<sup>2</sup>  
<sup>1</sup>aepawlak@ucalgary.ca, <sup>2</sup>eatond@ucalgary.ca

## ABSTRACT

The Hudson Bay basin is the least studied of the four major Phanerozoic intracratonic basins in North America, which include the hydrocarbon-rich Williston, Illinois and Michigan basins. Using azimuthal anisotropy results in conjunction with isotropic group velocity maps from previous work, we can further focus our study on determining the formation and regional crustal structure beneath Hudson Bay. Twenty-one months of continuous ambient-noise recordings have been acquired from 37 broadband seismograph stations that encircle Hudson Bay. These stations are part of the Hudson Bay Lithospheric Experiment (HuBLE), an international project that is currently operating more than 40 broadband seismograph stations around the periphery of Hudson Bay. The inter-station group-velocity dispersion curves found from noise-generated seismic-interferometry studies, also known as ambient-noise tomography, are input into a tomographic inversion procedure producing images of crustal azimuthal anisotropy. This study marks the first where ambient seismic-noise data have been considered in azimuthal anisotropy work.

## DATA

The data consists of three-component measurements of ground motion with a sampling rate of 40 samples per second. The dataset comprises 21 months of continuous data, starting from September 2006 and ending May 2008.

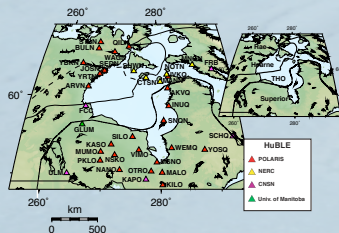


FIG. 1. Map of Hudson Bay showing all HuBLE stations using in this study. Black lines represent approximate location of tectonic boundaries (after Eaton and Darbyshire 2010).

## PROCESSING METHOD

Ambient-noise processing procedure follows the step described by Bensen et al. (2007).

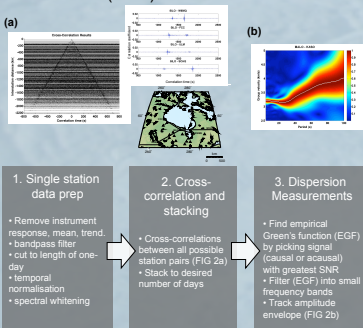


FIG. 2. (a) Stacked cross-correlations versus interstation distance for 591 two-station paths (left). Both positive (causal) and negative (acausal) lags are shown. Examples of five cross-correlations (upper right) illustrates asymmetry of correlograms with respect to signal-to-noise ratio (SNR), typical of this dataset. Corresponding paths are shown in the lower right. (b) Example time-frequency plot and dispersion analysis. The colour scale shows the amplitude envelope, normalised for each period value. The white line represents the group-velocity dispersion curve used as input for the inversion procedure.

## INVERSION

Tomographic inversion procedure follows the approach described by Darbyshire and Lebedev (2009). Using polar co-ordinates defined by  $\theta, \phi$ , the inversion problem is described by:

$$\iint K_l(\omega, \theta, \phi) \delta U(\omega, \theta, \phi) d\theta d\phi = \delta U(\omega) \pm \Delta U(\omega)$$

where  $\delta U(\omega, \theta, \phi)$  is the group-velocity perturbation at  $(\theta, \phi)$  and frequency  $\omega$ ,  $\delta U(\omega)$  and  $\Delta U(\omega)$  are the measured inter-station group-velocity anomaly and measurement error, respectively.  $K_l$  defines the sensitivity kernel for the  $l$ th station pair. For weakly anisotropic media, the Rayleigh velocity can be described as the sum of isotropic and anisotropic terms:

$$\delta U(\omega) = \delta U_{iso}(\omega) + A_1(\omega) \cos(2\Psi) + A_2(\omega) \sin(2\Psi) + A_3(\omega) \cos(4\Psi) + A_4(\omega) \sin(4\Psi)$$

where the '2Ψ' and '4Ψ' terms account for the  $\pi$ - and  $\pi/2$ -periodic variations, respectively, of velocity with wave-propagation azimuth  $\Psi$ .

## RESULTS

Preliminary results for 20s (left) and 30s (right) period are shown in FIG. 3. The 20s period is mainly sensitive to mid-crustal depths (~10-25 km), while 30s is sensitive to the lower crust (~20-35 km). We see lower velocities within the center of Hudson Bay, and higher velocities corresponding to the Archean Superior craton.

The 2Ψ anisotropy direction vary significantly between the 20s and 30s periods. The 20s period map is predominantly trending in a southwest-northeast direction, while the 30s period map has an almost north-south fabric. Results show weak correlation with regional tectonics. Note the 4Ψ signal is solely being used for testing robustness of the isotropic and 2Ψ results.

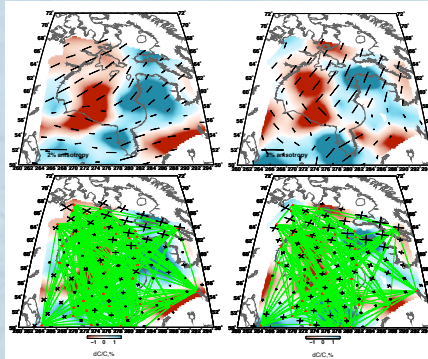


FIG. 3. Tomographic maps for periods 20s and 30s. Isotropic velocities show in red (lower velocity) and blue (higher velocity). The upper panels correspond with 2Ψ anisotropy directions, shown with the black lines. The lower panels show 4Ψ anisotropy with black crosses and green lines show inter-station paths for the given period.

## RESOLUTION TESTING

Two resolution tests have been done, results shown in FIG. 4. The first is an isotropic 'checkerboard' test, which checks for 'leakage' artifacts in 2Ψ anisotropy and isotropic patterns. The second test, rotates 2Ψ results by 90 degrees and is used to check for artifacts in 2Ψ anisotropy due to path coverage. Results for both tests are robust.

FIG. 4. Checkerboard reconstruction results for periods 20s and 30s (upper panel). Anisotropy resolution reconstruction results for periods 10s, 20s and 30s. To test for artifacts in the anisotropy results, the reconstruction results from FIG. 4 have been used, but the anisotropy results have been rotated by 90 degrees.

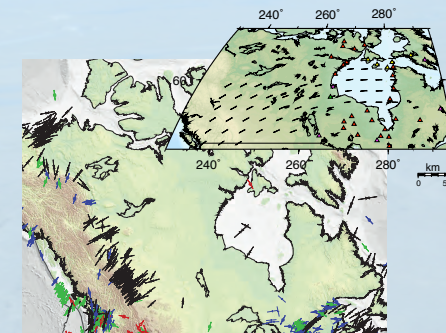
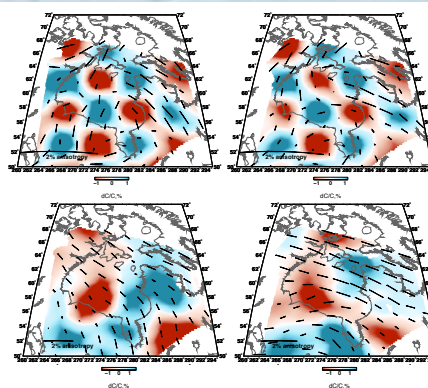


FIG. 5. World Stress Map (modified from Heidback et al. 2008) and plate motion direction map of Canada (inset) calculated using MORVEL 2010 (DeMets et al. 2010). Note the strong correlation between plate motion direction and axis of maximum compressive stress in Western Canada.

## CONCLUSIONS

- Results show weak correlation with regional tectonics.
- Our results have been compared with principle crustal stress data and plate motion directions (FIG 5). Crustal stress data is limited in this region and plate motion directions are inconsistent with our results.
- Other sources of stress perturbation may be required to explain our results, perhaps related to glacial isostatic adjustment.

## REFERENCES

Bensen, G.D., Ritzwoller, M.H., Barmin, M.P., Levshin, A.L., Lin, F., Moschetti, M.P., Shapiro, N.M. and Yang, Y., 2007. Processing seismic ambient noise data to obtain reliable broad-band surface wave dispersion measurements: *Geophys. J. Int.*, 169, 1351-1375.  
 Darbyshire, F.A. and S. Lebedev, 2009. Rayleigh wave phase-velocity heterogeneity and multilayered azimuthal anisotropy of the Superior Craton, Ontario; *Geophys. J. Int.*, 176, 215-234.  
 DeMets, C., R.G. Gordon, and D.F. Argus, 2010. Geologically recent plate motions. *Geophys. J. Int.*, 181, 1-80. doi:10.1111/j.1365-246X.2010.04491.x.  
 Eaton, D.W. and F.A. Darbyshire, 2010. Lithospheric architecture and tectonic evolution of the Hudson Bay region: *Tectonophysics*, 480, 1-22.  
 Heidback, O., M. Tingay, A. Barth, J. Reinecker, D. KerfeB and B. Muller, 2008. The World Stress Map database release 2008. Doi: 10.1594/GFZWSM.ReI2008.

## ACKNOWLEDGEMENTS

We are grateful to Dr. Honn Kao, from the Pacific Geoscience Center in Sydney, B.C., for providing us with initial data and assistance with data processing. A special thank you to Sergei Lebedev for allowing us to use his inversion code and Fiona Darbyshire for all her help with everything from helpful input to debugging code. We thank other members of the HuBLE working group for stimulating discussions and the CREWES project and CREWES sponsors at the University of Calgary for their support. Thank you to C-NGO and the First Nation communities around Hudson Bay for allowing seismometer deployments. This study was supported by NSERC through a Discovery Grant to DWE.